

# Communities and beyond: mesoscopic analysis of a large social network with complementary methods

Gergely Tibély,<sup>1</sup> Márton Karsai,<sup>2</sup> Lauri Kovanen,<sup>2</sup> Kimmo Kaski,<sup>2</sup> János Kertész,<sup>1,2</sup> and Jari Saramäki<sup>2</sup>

<sup>1</sup>*Institute of Physics and HAS-BME Cond. Mat. Group, BME, Budapest, Budafoki út 8., H-1111*

<sup>2</sup>*BECS, Aalto University, P.O. Box 12200, FI-00076*

(Dated: March 8, 2019)

Large complex networks show different levels of organization. At the mesoscopic scale communities are considered the most important structures that relate to system function but also other formations like trees or stars may appear. Communities are characterized as groups of nodes with dense internal and loose inter-group connectivity, but beyond this simple notion, even the definition of a community is a controversial issue. Numerous community detection methods have been proposed and assessed either on small empirical networks or larger synthetic benchmarks. However, little is known about their performance on large real-world networks and about the meaningfulness of the community structure they produce. Here we apply three community detection methods, Infomap, the Louvain method, and clique percolation to a large real-world social network based on mobile telephone calls and compare their results. Benchmarks are fabricated to capture only selected aspects of reality, while large empirical networks are much more complex. The Infomap and Louvain methods perform well on benchmarks but are found problematic in real-world networks as they lead to partitions, which on sparse graphs with large tree-like parts give rise to misleading conclusions. Clique percolation is found to outperform them by identifying at least the cores of communities, while some important connections nevertheless remain unidentified. The partitioning methods turn out to be useful in uncovering other mesoscale structures different from communities, such as large tree-like regions. The simultaneous application of different methods, the comparison of their similarities and differences with respect to topology, the density of links and the role of edge weights provide a more complete picture about the mesoscopic structure of large complex networks.

PACS numbers: 89.75.Fb, 89.75.Hc, 89.75.-k, 89.65.-s

Keywords: community detection; complex networks; social networks; mobile phone

## I. INTRODUCTION

### A. Background

Over the last decade or so, interdisciplinary research on complex systems has induced spectacular development of the field of complex networks [1–5]. It has become clear that diverse networks show similarities in their characteristics such as the degree distribution, average path length, and clustering coefficient. In addition, the structural properties of networks have been observed to have pronounced effects on dynamics of processes taking place on networks, such as spreading, diffusion, and synchronization [6–8]. For a comprehensive understanding of complex systems, the fundamental question is how the function of a system relates to the topology of the underlying network – in particular: are there topologically identifiable parts of the network that are responsible for specific functions? Large complex networks have different levels of organization, from microscopic dyads representing pairwise interactions to mesoscopic structures and finally to the network itself as a whole. Small-scale structures, *motifs*, have been extensively studied both for unweighted [9] and weighted [10] cases. So far, communities have attracted most attention among the mesoscopic structures, though other important mesoscale entities also exist. We are going to discuss them later in this paper.

*Community detection* is one of the key issues in this field and it aims at identifying dense clusters of nodes in networks<sup>1</sup>. This problem is far from trivial: even the definition of communities is a controversial issue. Moreover, the properties of the mesoscale structures make their detection a hard task. Also features such as hierarchical organization, where small communities reside inside larger ones, and overlapping communities, where a single node can participate in several communities, add to the complexity of this task. In addition additional complications arise if link weights are introduced, representing variable interaction intensity.

Under these circumstances, algorithms devised for this task must be on one hand accurate and on the other hand computationally efficient. Numerous community detection algorithms have been introduced [11] with different levels of accuracy and efficiency. Recently, systematic comparison of these algorithms has been initiated, based on benchmark networks with built-in community structure [12, 13]. Such benchmarks are an important tool in evaluating the performance of algorithms. However, benchmarks are unable to cover the whole complexity of large complex networks. It is therefore of central importance to compare community detection algorithms not

---

<sup>1</sup> In this paper, the words “community”, “group” and “cluster” will be used as synonyms for those dense clusters.

only on benchmarks, but also on large real networks. This is the goal of the present paper.

The first propositions for detecting communities were based on methods borrowed from other disciplines, such as agglomerative and divisive hierarchical clustering [14, 15] which is frequently used e.g. in genetics-based population biology. For selecting the “correct” level of divisive clustering, Ref. [16] defined *modularity*, which quantifies the quality of a partition. Later it was realized that divisive clustering can be replaced by any method which maximizes modularity. As this requires a search in a space which is hopelessly large for an exhaustive algorithm, several different heuristics have been proposed [11]. In fact, it has been proven that the exact treatment of the task is an NP-complete problem [17]. Currently, the theoretical background of modularity has been more or less completed [18, 19]. It has been found that there is a fundamental bias [20, 21], namely, that modularity optimization is biased towards large communities, even when they clearly contradict common sense. Despite this bias, modularity optimization has become one of the most widely applied methods.

At the same time, methods based on entirely different principles have also been introduced, such as *clique percolation* [22], which is a fully deterministic local method based on rolling cliques, *i.e.* fully connected subgraphs, on the network.

## B. Goals of this work

Community detection methods have so far been tested either on very small graphs ( $\mathcal{O}(10^2)$  nodes) or more recently, on larger synthetic networks [29]. Only few methods have been applied on large networks [28–31]. The lack of knowledge of the performance of community detection methods on large graphs is mainly due to three reasons. First, communities are easily visible in visualizations of small networks<sup>2</sup> and hence results can be qualitatively judged by observation, while the size and complexity of large networks makes evaluation of community detection results difficult. Second, the recently introduced synthetic benchmarks with built-in community structure [12, 13] only account for the heterogeneous distributions of node degrees and community sizes, leaving out properties such as assortativity [32], distribution of motifs [33], the existence of cliques [22] and overlapping communities [34]. Third, many algorithms are too slow for graphs of considerable size ( $N \gtrsim 10^6$  nodes) [29]. However, several networks of interest fall in this size range — e.g. data on the WWW, electronic footprints of millions of mobile

phone or instant messaging users, and networks of social web such as Facebook.

In this paper, we apply selected community detection methods on a large real-world social network to investigate the differences between detected community structures. As our network is very large, computational performance is a very important factor in the choice of methods; any method whose running time grows faster than linear in the number of nodes is thus excluded. In addition, we wish to use methods that have been shown to detect meaningful communities in benchmark graphs.

Our selection consists of three methods. The *Infomap* method (IM) introduced by Rosvall *et al.* [25] provides a fast solution for community detection on large graphs, and has been found to perform best on a state-of-the-art benchmark [29]. The *Louvain* method (LV) [30] represents the widely used family of modularity optimization methods. This method is very fast, and has also been successful on benchmarks [29], being the best among modularity optimization variants. The third method *clique percolation* (CP), has the advantage of allowing for overlapping communities. It has been observed to perform less well on benchmarks [29]; however, CP is designed to detect dense communities consisting of adjacent cliques, whereas the benchmark communities are in essence Erdős-Rényi networks and thus contain only few cliques. As the empirical test network, we have chosen a large network with millions of nodes, constructed from mobile phone call records [35]. This choice enables us to relate the present findings to the known characteristics of the societal-level network [35]. In earlier studies, it has been seen that the overlap between the neighborhoods of the two end nodes of a link is an increasing function<sup>3</sup> of the link weight [36], in accordance with the “weak ties” hypothesis of Granovetter [37], a feature which should be reflected in correlations between link weights and communities. We also study structural features of communities in order to judge whether the detected communities are meaningful in the context of social networks, and address the issue of hierarchy, *i.e.* whether communities detected by one method are the building blocks of communities detected by another method.

At this point we like to anticipate some of the results. It will turn out that for large, sparse networks community detection methods based on partitioning the whole graph lead to a large number of false communities in the sense that they cannot be considered as communities by any reasonable definitions. The question raises: Do the identified regions have any mesoscopic structural meaning? In fact, there are such structures beyond communities, like large tree-like parts or star-like formations. We will show that the simultaneous application of different methods is helpful in identifying them.

<sup>2</sup> Note that, however, there is no “correct” way of visualizing a graph, and the commonly applied spring-charge-algorithms tend to produce layouts where densely interconnected sets of nodes cluster together.

<sup>3</sup> With the exception that the overlap decreases for the very strongest 5% of links.

The paper is organized as follows: in Section II, we describe our choice of community detection methods and the data set used. In Section III, we discuss statistics and topological features of detected communities and relationships of edge weights to community structure. In Section IV, we quantify the differences between communities with a pairwise comparison of methods. Finally, in Section V we present conclusions.

## II. METHODS

### A. The dataset

The empirical test network used in the following comparisons is a large mobile phone call network (MCN) based on call billing records of seven million individual customers of one operator covering about 20% of the population of a country. These records are taken over a period of 18 weeks (126 days) for privacy, the identities of the customers have been replaced by surrogate keys. For our study, we keep only voice calls and filter out all other services such as text messages, and also exclude calls with customers of other operators.

Furthermore, we consider only mutual social relations by filtering out one-way calls by requesting at least one reciprocated call over the 18-week period. Thus we obtain a static mutual network (SMN) with  $N = 5.3$  million nodes and  $L = 11.1$  million links, where the vast majority of nodes belong to the largest connected component (LCC) of size  $N_{LCC} = 4.9 \times 10^6$  with  $L_{LCC} = 10.9 \times 10^6$  links (mean degree  $\langle k \rangle \approx 4.44$ ). The second-largest connected component has only 47 nodes so consequently, we use only the LCC (referred to as *the network*) from here on. For comparing unweighted and weighted methods, we constructed a network without edge weights, and a network with weights  $w$  defined as the sum of call durations (in seconds) between two customers. The average edge weight in the LCC is  $\langle w \rangle \approx 4634$ .

### B. Community detection methods

In the following, we will give a brief description of each chosen method; for details, the reader is referred to the original publications.

*The Louvain method* (LV) is based on partitioning the network into non-overlapping communities by maximizing the modularity

$$Q = \frac{1}{2m} \sum_{i,j} \left[ A_{ij} - \frac{k_i k_j}{2m} \right] \delta(c_i, c_j), \quad (1)$$

where  $A_{ij} = 1$  if there is an edge between  $i$  and  $j$  and 0 otherwise,  $k_i = \sum_j A_{ij}$  is the degree of vertex  $i$ ,  $c_i$  is the index of the community to which vertex  $i$  is assigned, and  $m = \frac{1}{2} \sum_{i,j} A_{ij}$  is the number of edges in the network. This method can be used for weighted networks

by replacing the adjacency matrix  $A_{ij}$  with a weight matrix  $W_{ij}$ , whose element  $w_{ij}$  represents the weight of the edge between  $i$  and  $j$ . Modularity represents the difference between the observed numbers/total weight of edges within communities and their expected values in a random reference. However, LV does not strive for globally optimizing modularity; instead it uses a greedy algorithm where initially all nodes are assigned to separate communities and then in random order merged with neighboring communities so that the modularity increases maximally at each step. Since the order in which the nodes are processed is random, the method is stochastic. This step is iterated until a local optimum is found. This local scheme seems to avoid some of the resolution issues of modularity. Next, each community is shrunk into a “super-node”, and the whole procedure is recursively repeated on the “renormalized” community graph until no further improvement in modularity is possible. The algorithm then returns a partition of the original graph. This renormalization-like procedure makes the method very fast, as most of the running time is concentrated on the first few renormalization steps. A further advantage is that the super-node sets can be associated with hierarchical levels of communities. Code for the algorithm is available for download [38].

*The Infomap method* (IM) also yields a partition of the network. IM minimizes a fitness function corresponding to the description length of a random walk on the network. Random walks are described using a two-level coding: the higher level has a single codebook for communities, and on the lower level each community has one codebook (with a special exit code for moving out of the current community). In the solution with the minimum description length the partition to communities is chosen so that random walks tend to remain within communities for longer periods of time, and events where the walk crosses over from one community into another are less frequent: the code lengths reflect the frequency of a random walker being located in a community or node. The optimization balances frequency of movement between communities with community size: too small communities increase the description length due to the higher frequency of community crossings, and communities containing too many nodes require a longer description. As with modularity based methods, an exhaustive search for the optimal partition is not feasible and therefore Infomap employs a deterministic greedy search algorithm followed by simulated annealing. Infomap can also be used in weighted networks. In this case random walks are biased towards edges of higher weight, corresponding to the assumption that edges residing inside communities have in general larger weights. Infomap is also available for download [39].

*The clique percolation method* (CP) is a deterministic method which defines communities as percolation clusters of adjacent fully connected subgraphs, i.e. cliques. Cliques of size  $k$  are defined to be adjacent if they have  $k - 1$  nodes in common. Different values of  $k$  hence yield

different community structures, such that communities obtained using a larger value of  $k$  necessarily reside inside communities obtained for smaller values of  $k$ . The typical way of applying the method, as originally suggested in Ref. [22], involves choosing the value of  $k$  as smallest value for which there is no percolating cluster, *i.e.* a community whose size is of the order of network size. Because of the way  $k$ -clique communities are defined, clique percolation does not yield a community partition where each node belongs to a single community. Instead, it allows for overlapping communities, *i.e.* nodes may simultaneously belong to more than one community. Furthermore, if nodes do not participate in  $k$ -cliques, they are not assigned to any community. Both properties are very “physical”: sparse regions of the graph do not appear as communities, and, *e.g.*, members of a social network usually belong to several group simultaneously, such as family, friends, and colleagues.

The clique percolation method has also been extended for weighted networks [42]. In addition to topological  $k$ -cliques, weighted clique percolation (wCP) takes into account the *intensity* [10] of cliques, defined as

$$I(\mathcal{C}) = \left( \prod_{\substack{i < j \\ i, j \in \mathcal{C}}} w_{ij} \right)^{2/(k(k-1))} \quad (2)$$

where  $w_{ij}$  denotes the weight of the edge between nodes  $i$  and  $j$ . In wCP, only cliques whose intensity exceeds a threshold are considered and communities are defined as sets of adjacent  $k$ -cliques for which  $I > I_c$ . Similarly to selecting the proper value of  $k$ , the intensity threshold  $I_c$  is chosen such that as many nodes as possible participate in communities, yet there is no percolating community. Thus, one looks for the critical percolation point using  $I_c$  as the control parameter [42] and sets the intensity threshold slightly below the critical point. The critical point can be identified by the point of sharp maximum of the susceptibility-like quantity

$$\chi = \sum_{S_\alpha \neq S_{max}} S_\alpha^2 / \left( \sum_\beta S_\beta \right)^2 \quad (3)$$

where  $S$  stands for the community size, and  $\alpha$  and  $\beta$  index the communities.

### C. Notes on applying the methods

*The Louvain method.* As the LV agglomeratively builds larger communities until no improvement in modularity can be achieved and its application to our data yielded very large communities with sizes up to  $S \simeq 5 \times 10^5$  nodes, both for the weighted (wLV) and unweighted (LV) cases. We adopted the view that the different renormalization levels correspond to the different levels of hierarchical organization. To obtain meaningful, smaller-scale social groups and to be able to compare results with other methods, we chose to use the method at the first level,

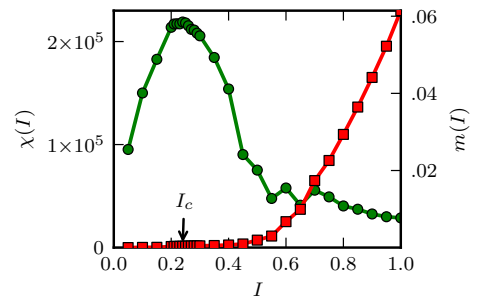


Figure 1: Order parameter  $m(I)$  ( $\square$ ) and susceptibility  $\chi(I)$  ( $\circ$ ) as a function of the control parameter, intensity threshold  $I$ , for determining the critical intensity threshold for weighted clique percolation with  $k = 3$ . The phase transition point is located at  $I_c \approx 0.24$ .

*i.e.* before the first merger of communities was made. This step, however, revealed another feature of the LV method: while the modularity value is quite similar regardless of the order the nodes are processed, for example the size of the largest community varies greatly. For our purposes we use a community partition where the size of the largest community is around  $10^3$ , since this makes sense in the social context. Because LV is essentially a local method and we are dealing with a very large network, it is reasonable to assume that the statistical properties of the partitions are on average similar and do not vary as much as the size of the largest community. In addition the LV algorithm can in some cases produce *disconnected* communities. Only few such communities were encountered, and we dealt with this by turning each connected component into a community.

*The Infomap method.* The Infomap method was applied directly as it is.

*Clique percolation.* For the unweighted CP, one needs to choose the proper value of  $k$  to yield communities such that there is no percolating cluster. For the mobile network setting  $k = 3$  gives rise to percolating community but choosing  $k = 4$  breaks it to meaningful community division. For the weighted CP, however, one has to also choose the threshold intensity  $I_c$ . For this our approach was to select  $k = 3$ , since the percolating cluster will fragment once the proper threshold is applied. We varied the intensity threshold  $I_{>}$  while monitoring the order parameter  $m(I_{>})$  and the susceptibility  $\chi(I_{>})$  defined in Eq.3. Figure 1 displays the results. At the critical phase transition point  $I_{>} = I_c$ , a giant cluster emerges, while susceptibility diverges if the system is infinite, or shows a pronounced peak if the system is finite. As seen in Fig. 1, this happens around  $I_c \simeq 0.24$ , which was chosen as our intensity threshold. For CP and wCP, we applied the fast algorithm introduced in [43].

The running times of all the algorithms used are displayed in Table I below. It is evident that while LV and CP are fast with runtimes of the order of minutes, Infomap exceeds these by far, requiring several days to complete. All runs were done on a standard desktop machine,

Table I: Running times of the different algorithms on our data set of  $N = 4.9 \times 10^6$  nodes and  $L = 10.9 \times 10^6$  links.

	unweighted	weighted
Louvain	2 min 7 s	1 min 30 s
Infomap	46 h 44 min	3 h 20 min
Clique percolation	2 min 10 s	4 min 52 s

utilizing a single processor.

### III. RESULTS

#### A. Community size distributions

We begin our investigation by looking at community size distributions. Earlier results suggest that the community size distributions are typically broad [22, 31, 44]. Such is the case here as well, as can be seen in Figs. 2 a), c), and e), where the left panels display community size distributions  $P(S)$  for all methods, for weighted and unweighted cases.

For IM, the tail of the distribution appears power-law-like (Fig. 2 a), with an estimated exponent of  $\alpha_{IM} \simeq -2.7$ . However, there is a peak in the beginning of the distribution, as communities with very small sizes are rare. A feasible explanation of this is that IM assigns high-degree vertices to larger communities, so that the smallest communities are (often treelike) groups of “left-over nodes” of lower degree and connected with single links to other communities (see Fig. 3). For wIM with weights, the community structure appears different – the distribution is monotonously decreasing, and its tail can be approximated with a power-law with an exponent of  $\alpha_w \simeq -5.7$ ). Hence the weighted communities are on average smaller.

For LV and wLV, the tails of the distributions behave similarly to IM and wIM (Fig. 2b). Here the largest clusters are about one order of magnitude smaller than for IM, but the power-law exponents roughly characterizing the tails of the distributions are similar,  $\alpha_{LV} \simeq -3.0$ , and  $\alpha_{wLV} \simeq -5.7$ . The main difference for IM is that small unweighted communities are well presented here, and the unweighted distribution is also monotonically decreasing.

Finally, for CP and wCP, we can beforehand expect that the community size distributions are close to power laws, as the clique clusters are detected close to the critical point where a giant community would emerge. This is indeed the case as depicted in Fig. 2c). The only apparent difference is that the largest weighted communities are larger than the largest unweighted communities. This is because 3-cliques are used for weighted communities and 4-cliques for unweighted communities. Although these communities partially overlap (see Sect. IV), 3-clique communities extend far beyond 4-clique communities.

Earlier, link weights have been seen to correlate with

the topology of social networks, such that high-weight links are associated with dense local neighbourhoods [35, 36]. At least for the partition-based methods, this would imply that unweighted communities should split into smaller weighted communities when the weights are taken into account. This is in line with the above observations on community size distributions. For a more detailed view, we have investigated how the largest unweighted communities relate to weighted communities. For this, we focused on the 5 largest unweighted communities detected by each method, and for each of them, we investigated the sizes of weighted communities to which their constituent nodes are assigned. For IM and LV, nodes in large unweighted communities are split among many weighted communities whose size distribution is broad. For CP, nodes of unweighted communities participate in weighted communities that can be much larger than any unweighted community.

#### B. Visual observation of small communities

Next, we use network visualization for a qualitative overview of the structural properties of communities produced by each method. Fig. 3 shows archetypal unweighted communities of small sizes  $S = 5, 10, 20$ , and 30, and their immediate network surroundings. We have resorted to small sizes, since larger communities tend to be too complex for two-dimensional visualization.

The topology of CP communities is not surprising since they are forced to consist of 4-cliques. It is also apparent that the neighbourhoods of CP communities are clustered, which indicates the presence of structural correlations in the network. LV communities in this size range contain many interconnected cliques, which coincides well with the general idea of social groups. On the other hand, Infomap communities appear much more treelike. A typical IM community with  $S \leq 10$  is a tree or almost a tree, located at the “edge” of the network, in the sense that the community is connected to the rest of the network by very few links. Treelike communities do not fit well neither with the view of social groups or the general idea of communities which makes this feature of Infomap in this context problematic. However, if a network contains treelike regions, partition-based methods will correspondingly yield treelike communities, as also seen in Ref. [31]. This is true for the LV method as well (see Sect. IV), which appears to “tile” the treelike IM communities with very small treelike communities ( $S \simeq 2 \dots 3$ , see Sec. IV B). If the call network is interpreted as a proxy of the underlying “true” social network, the abundance of treelike parts should be viewed as an artifact related to sampling, *i.e.* the fact that our sample does not cover 100% of the population. Nevertheless, empirical data is rarely perfect, and any reasonably community detection method should deal with this in a sensible way. One could argue that in treelike regions the network is so sparse that there is no information about community

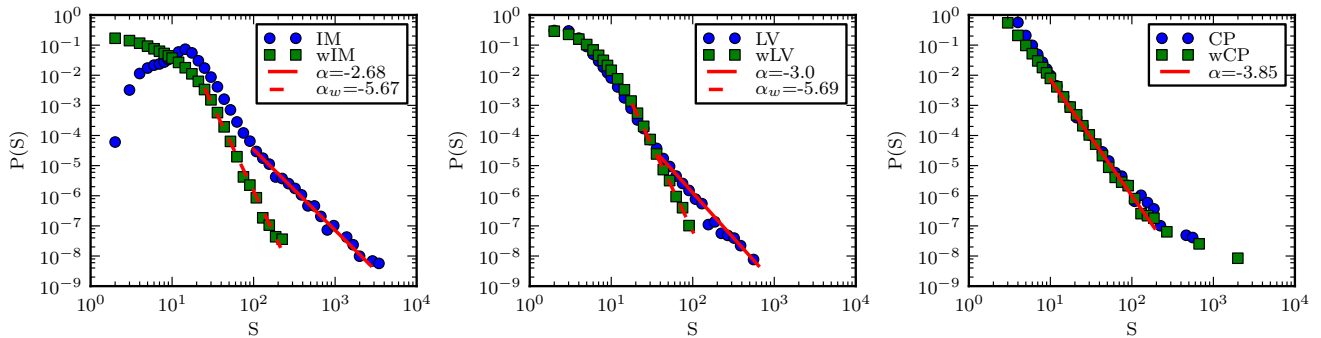


Figure 2: Community size distributions for IM, LV and CP and their weighted versions.

structure. Thus, CP’s requirement for nodes to participate in a clique to be assigned to any community, which has been seen as problematic under some circumstances, appears meaningful here. However, the treelike structures detected by the partition-based methods are real and provide a lot of information about the mesoscopic structure of the network (see Fig. 5).

Figure 4 shows typical weighted communities, and roughly the same remarks hold as for the unweighted case. When the weights are taken into account, the partition-based methods tend to produce even more tree-like communities, which have the appearance of local “backbones” of the network. While this is a natural consequence of the way wIM and wLV take the weights into account, yet again such communities do not coincide well with the idea of dense social groups.

### C. Community density distribution

As treelike communities were observed above, we next turn to quantitative characterization of community densities. The density of a subgraph, such as a community, is defined as the proportion of edges out of all possible edges,  $D_c = L_c / [\frac{1}{2}S(S-1)]$ . However, as communities must necessarily be connected subgraphs, they need to have at least  $S-1$  edges. Thus, similarly to Ref. [31], we define community edge density relative to the number of links in a tree:  $D_c^{\text{rel}} = L_c / (S-1)$ . Then  $D_{c,\text{min}}^{\text{rel}} = 1$  if the community is a tree, and  $D_{c,\text{max}}^{\text{rel}} = S/2$  if the community is a clique. Note that for CP, the smallest possible density is reached when each new node in the  $k$ -clique community adds only  $k-1$  edges, and thus  $L_c = \binom{k}{2} + (k-1)(S-k)$  which gives  $D_{c,\text{min}}^{\text{rel}} = (k-1)(S - \frac{k}{2}) / (S-1)$ . For  $S \gg k$  this is approximately  $k-1$ .

Figure 6 shows the distributions and average values of  $D_c^{\text{rel}}$  for each community size for CP, IM and LV. It is seen that in all cases, the average values of  $D_c^{\text{rel}}$  reside between the two extremes. As expected, CP yields the densest communities. Comparing the distributions for IM and LV for  $10 < S < 20$  confirms our earlier observation that there are more treelike communities in IM than in LV, as the IM distribution values remain high down to

Table II: Fraction of edges inside communities ( $L_c/L$ ), between communities ( $L_{c-c}/L$ ), between community nodes and nodes excluded from all communities ( $L_{c-n}/L$ ), and between nodes excluded from all communities ( $L_{n-n}/L$ ). Here  $L$  denotes the number of edges in the GCC of the mobile call graph.

	$L_c/L$	$L_{c-c}/L$	$L_{c-n}/L$	$L_{n-n}/L$
IM	0.682	0.318	0	0
LV	0.513	0.487	0	0
CP	0.214	0.055	0.256	0.476
wIM	0.558	0.442	0	0
wLV	0.448	0.552	0	0
wCP	0.186	0.077	0.307	0.430

$D_c^{\text{rel}} = 1$ . It is also seen that for  $S < 10$ , IM communities are indeed very often trees. For LV the distribution has a curious bimodal shape when  $20 < S < 50$ : while typical LV communities of this size have  $D_c^{\text{rel}}$  around 2–4, there is a small number of LV communities that are trees ( $D_c^{\text{rel}} = 1$ ) but none that are almost trees. Taking a closer look at these trees reveals that they are in fact stars. Again, whether stars alone should qualify as social communities is debatable.

The plots for weighted communities in Fig. 6 show that weights make the community densities behave more similarly. It is also clear that IM and LV communities become more treelike, as pointed out before.

### D. Intra- and intercommunity edges

Let us next focus on edges and their relationship to community structure. We categorize edges into different groups: intra-community edges ( $L_c$ ) connect nodes of the same community, while inter-community edges ( $L_{c-c}$ ) join nodes of different communities. For CP, there are also edges connecting community nodes to nodes which do not participate in communities ( $L_{c-n}$ ) and edges connecting the latter type of nodes ( $L_{n-n}$ ). Relating the numbers of intra- ( $L_c$ ) and inter-community edges ( $L_{c-c}$ ) to the total  $L$  number of edges (Table II) one can see that a larger

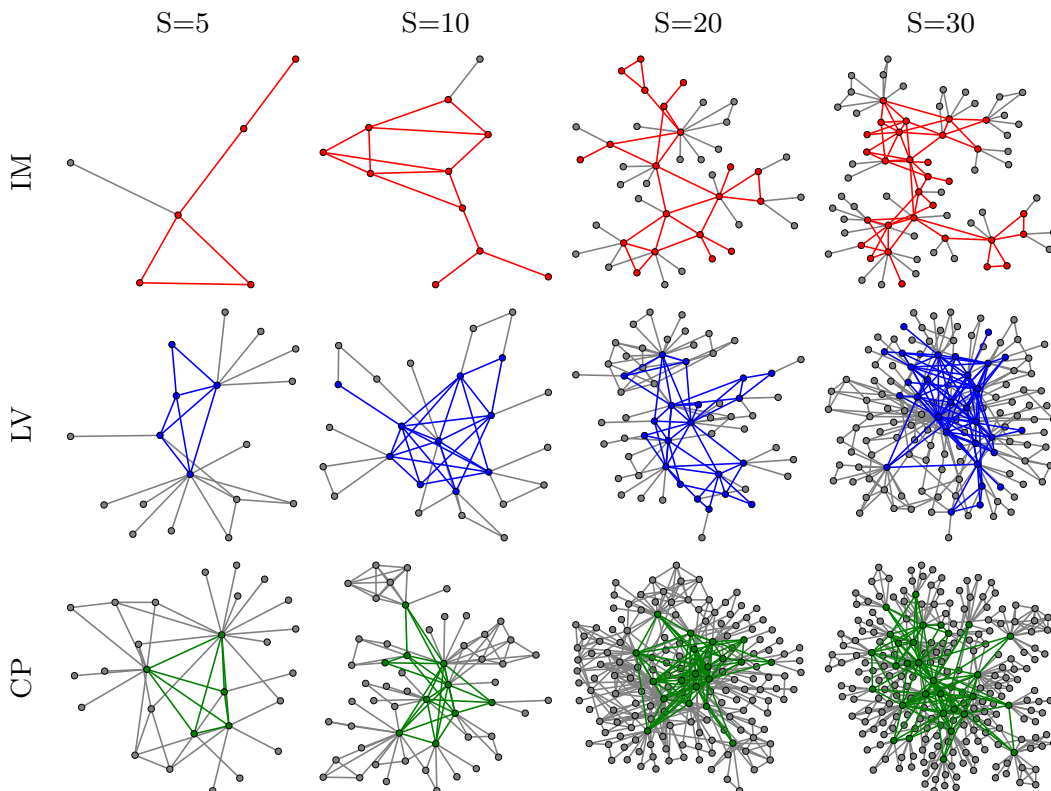


Figure 3: Typical unweighted communities of different size. These examples have been selected by hand from a large random sample of communities of a given size with the intention of presenting archetypal examples. The colored nodes and edges denote nodes inside a single community, and the gray nodes are the first neighbors of the nodes in the community.

Table III: Ratio of average edge weights belonging to different edge sets to the network average.  $\langle w \rangle$  denotes the average edge weight of the LCC of the network,  $\langle w_c \rangle$  is the average weight of edges inside communities,  $\langle w_{c-c} \rangle$  between communities,  $\langle w_{c-n} \rangle$  between community nodes and excluded nodes, and  $\langle w_{n-n} \rangle$  between excluded nodes.

	$\langle w_c \rangle / \langle w \rangle$	$\langle w_{c-c} \rangle / \langle w \rangle$	$\langle w_{c-n} \rangle / \langle w \rangle$	$\langle w_{n-n} \rangle / \langle w \rangle$
IM	1.14	0.69		
LV	1.20	0.78		
CP	1.20	0.57	0.80	1.06
wIM	1.65	0.18		
wLV	1.92	0.25		
wCP	2.57	0.43	0.57	0.73

fraction of edges is located inside communities than between communities for all methods. This is as expected, since communities should be groups of nodes with dense internal connections. All methods yield a community division that is correct in this respect.

In earlier studies of the MCG [35, 36], it was seen that low-weight edges are associated with little overlap between the neighbourhoods of the two nodes. Strong edges were seen to be associated with overlapping neighbourhoods. Such weight-topology correlations are in agree-

ment with the Granovetter hypothesis[37]. As communities by definition imply overlapping neighbourhoods, we can expect that the links interconnecting communities should on average be weaker than those within communities. Table III displays the ratio of the average weight  $\langle w_* \rangle = \sum_{w_*} wL(w)/L$  of intra- and inter-community edges to the whole network average  $\langle w \rangle$  for all methods<sup>4</sup>. It is evident that in all cases, communities on average contain stronger ties, while edges linking communities are weaker, in agreement with earlier results. Note, however, that the weighted methods a priori assume that communities have strong edge weights, and thus it is not surprising that for wIM, wLV, and wCP, the difference between intra- and intercommunity edge weights is larger.

In order to obtain more insight beyond averages, we have investigated the average weights of edges as function of community size. Fig. 7 displays the average weights of edges inside communities as function of community size, such that the weights have been normalized by the network average. For unweighted methods, small communi-

<sup>4</sup> For unweighted methods, the communities were extracted without using the edge weights; the weights were taken into account only in the subsequent analysis.

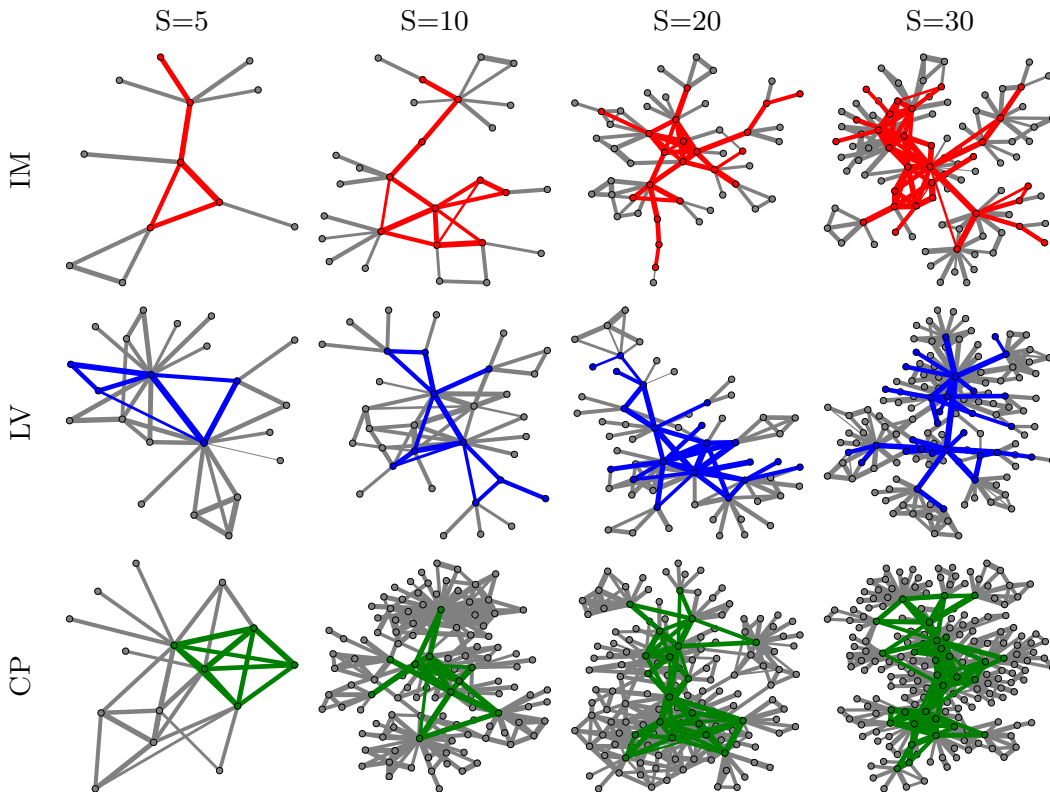


Figure 4: Typical weighted communities of different size. The edge width denotes link weight.

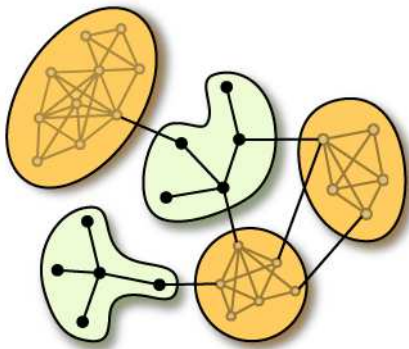


Figure 5: A schematic illustration of the observed mesoscopic features. While all methods find (some) dense regions, *i.e.* communities in the usual sense, the network also contains regions which are trees or treelike. Partition-based methods (IM and LV) construct treelike communities of nodes in such regions, while CP only assigns nodes in the denser regions to communities.

ties that represent the majority of communities contain edges with weights slightly above the network average. However, the average edge weights of large communities ( $S \gtrsim 50 - 100$ , depending on the method) are slightly below the network average. This is an expected conse-

quence of the large number of small communities with high weights. For weighted methods, the community-internal edge weights behave differently. For wCP, average community edge weights are always above network average. For wIM and wLV, weights are above network average, except for few largest communities.

#### IV. PAIRWISE COMPARISONS

We will conclude our analysis by directly comparing the communities calculated with different methods. This comparison will be done pairwise, for the pairs IM-CP and IM-LV and between their weighted versions. We will also compare the community structures obtained from applying the weighted and unweighted versions of each method.

##### A. Neighbourhood overlap

The first tool we employ for comparing two community structures is the *neighbourhood overlap*. It quantifies the extent of similarity of the neighbourhood of a node regarding the community structure. Let  $n(i, m_j)$  be the set of  $i$ 's neighbours which are members of the same community as  $i$  itself, as obtained by applying method  $m_j$ . We



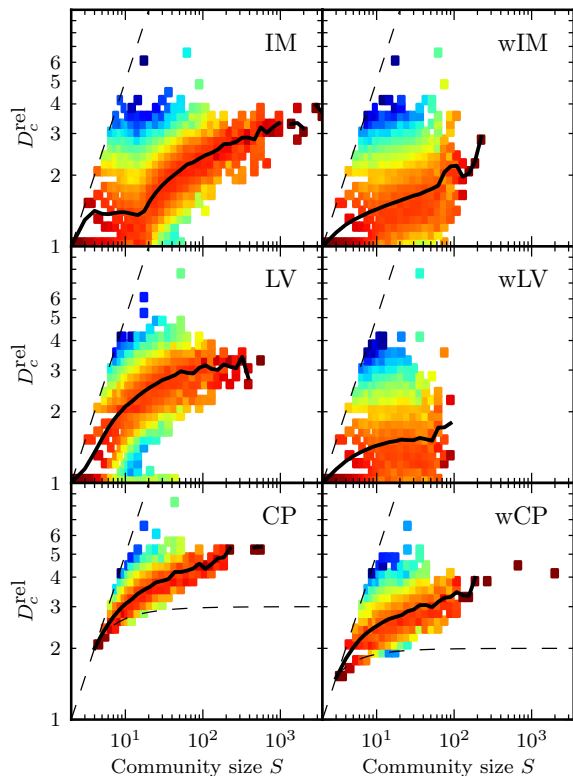


Figure 6: The distribution of relative density  $D_c^{\text{rel}} = L_c/(S - 1)$  for communities from each method. In all plots, each column represents a distribution and is normalized to one, the colors indicating probability density. The thick solid line shows the average  $D_c^{\text{rel}}$  for all communities of a given size. The dashed straight line corresponds to cliques, for which  $L_c = \frac{1}{2}S(S - 1)$  and thus  $D_c^{\text{rel}} = S/2$ . For IM and LV the smallest density is 1, which corresponds to trees. For CP, the smallest possible density is indicated by the curved dashed line (see text).

define the neighbourhood overlap as the Jaccard index of  $n(i, m_1)$  and  $n(i, m_2)$ :

$$O(i, m_1, m_2) = \frac{n(i, m_1) \cap n(i, m_2)}{n(i, m_1) \cup n(i, m_2)}. \quad (4)$$

Hence  $O = 1$  if exactly the same neighbours of  $i$  belong to its own community for both methods  $m_1$  and  $m_2$ , and  $O = 0$  if the sets do not overlap. In the case of CP, we only calculate this measure for nodes which participate in at least one community; for nodes which participate in several, we assign the node to the community where most of its neighbours reside.

Figure 8 a) displays the average neighbourhood overlap as a function of degree for the pairs IM-CP, IM-LV, and their weighted versions. It is clearly seen that there are large differences between the methods. We find a decreasing trend for all the pairs, which indicates that the community neighbourhoods of low-degree nodes tend to be more similar across the methods, up to  $O = 1$  which

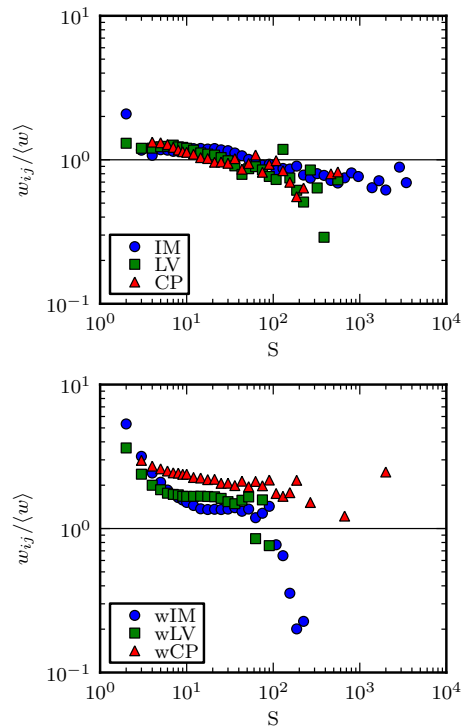


Figure 7: Average edge weights  $w_{ij}/\langle w \rangle$  inside communities as a function of community size  $S$ , normalized by the network average.

in turn indicates exact similarity, whereas the neighbourhoods are fairly dissimilar for nodes of higher degree. Neighbourhoods match on average best between the weighted Infomap and weighted Louvain methods; as expected and wIM and wCP turned out to be most dissimilar, as the underlying philosophies of these methods are very different, and the large number of nodes appearing in any CP community reduces the neighbourhood overlap. However, for low  $k$ , the overlap is surprisingly good. It is also worth noting that unlike for the IM-CP and its weighted counterpart pair, taking the weights into account increases the neighbourhood overlap between IM and LV, indicating that there are similarities in their response to weight-topology correlations.

Let us next compare the unweighted methods to their weighted counterparts (Fig. 8b). Here, the neighbourhood overlap between CP and wCP behaves very differently from the other pairs and is especially low for low-degree nodes. This is because wCP is based on 3-cliques, and even after intensity thresholding, there is a large number of nodes participating in 3-clique communities which are entirely outside the unweighted 4-clique communities. For IM and LV the overlap decreases to fairly low values with increasing  $k$ , which indicates that taking weights into account considerably changes the resulting community partitions.

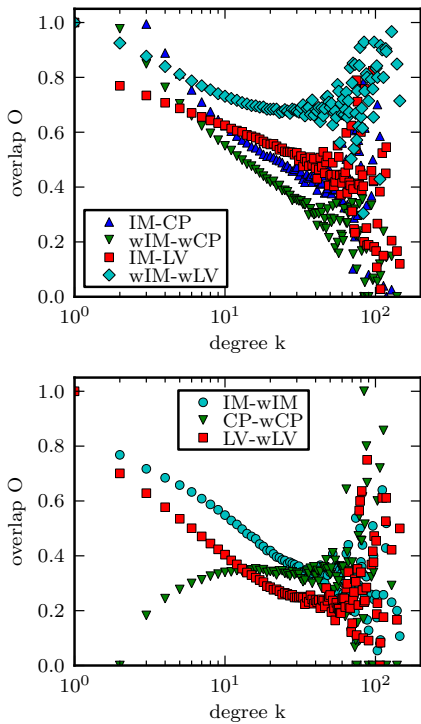


Figure 8: Average neighbourhood community overlap  $O$  as a function of node degree  $k$ , for the method pairs (Left) IM-CP (solid squares), wIM-wCP (open squares), IM-LV (solid circles), and wIM-wLV (open circles) (Right) CP-wCP (circles), IM-wIM (squares), and LV-wLV (diamonds).

### B. Nested communities: tiling and inclusion imperfection

As our final comparison, we will assess the extent to which communities detected with one method contain communities of the other. Such nested communities reflect hierarchical community structure, and in theory, different methods could detect communities at different levels of hierarchy. We quantify the nestedness of communities by two measures. The *tiling imperfection* measures how perfectly the communities of method  $m_1$  can be tiled by communities of  $m_2$ . Let  $c_{i,1}$  be a community detected by method 1, with size  $S_i$ . We define the tiling imperfection for  $c_{i,1}$  with respect to method 2 as

$$I(i, m_1, m_2) = \frac{F_{i,int} + F_{i,ext}}{S_i}, \quad (5)$$

where  $F_{int}$  and  $F_{ext}$  are numbers of internal and external *faults*, respectively. The faults are defined as follows: first we define the covering set  $C_2$  as the subset of communities detected by  $m_2$  sharing at least half of their nodes with  $c_{i,1}$ . Then, any node belonging to  $c_{i,1}$  which is not covered by any of the nodes in  $C_2$  is counted as an internal fault. Furthermore, any nodes in  $C_2$  which do not reside inside  $c_{i,1}$  are counted as external faults. If the communities of  $C_2$  perfectly tile the community  $c_{i,1}$ , then  $I(i, m_1, m_2) = 0$ .

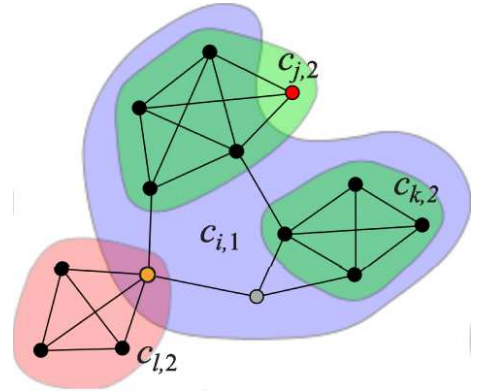


Figure 9: A schematic illustration of tiling and inclusion imperfection.  $c_{i,1}$  is the focal community of size  $S_i = 10$ , detected by method 1 (light blue shading). The covering set  $C_2$  includes  $c_{j,2}$  and  $c_{k,2}$  detected by method 2, as half of their nodes reside within  $c_{i,1}$ . Community  $c_{l,2}$  is excluded because the majority of its nodes are outside  $c_{i,1}$ . The gray node does not belong to any community detected by method 2. For tiling imperfection, the total number of internal and external faults is 3 (external: red node, internal: orange and gray nodes) and hence  $I_{i,m_1,m_2} = 3/10$ . For inclusion imperfection, only the orange node is counted as an internal fault, and hence  $I_{i,m_1,m_2}^* = 2/10$ .

As CP and the partition-based methods have the fundamental difference that unlike for IM and LV, all nodes are not assigned to a community in CP, we define another measure of nestedness for this special case. If  $m_1$  is partition-based and  $m_2$  is CP, some nodes in  $c_{i,1}$  may not belong to any of the communities of  $m_2$ . Nevertheless, the set  $C_2$  might be perfectly contained within  $c_{i,1}$  – e.g., consider the LV community with  $S = 5$  in Fig. 3, which contains a 4-clique (community). For characterizing this, we define the *inclusion imperfection*  $I^*$  similarly to the tiling imperfection (Eq. 5), with the following difference: nodes of  $c_{i,1}$  can be counted as internal faults *only* if they belong to some community of  $m_2$ . See Fig. 9 for a schematic depiction.

Figure 10 displays both imperfection measures for the IM-CP and IM-LV pairs as a function of community size. The IM-CP tiling imperfection curve (panel a) shows that especially small IM communities are only very poorly tiled by CP communities. In the light of the results presented for community densities, this is evident, as small IM communities are either treelike or contain treelike parts whose nodes cannot be covered by any CP community. However, the inclusion imperfection values are fairly low, again especially for small communities. This means that if there are nodes within IM communities which belong to CP communities, the latter tend to remain within the boundaries of the respective IM communities. This finding is corroborated by the CP-IM tiling imperfection values, measuring how well CP communities can be tiled by IM communities. In this case, the tiling imperfection values are very high; in conjunction with the result that

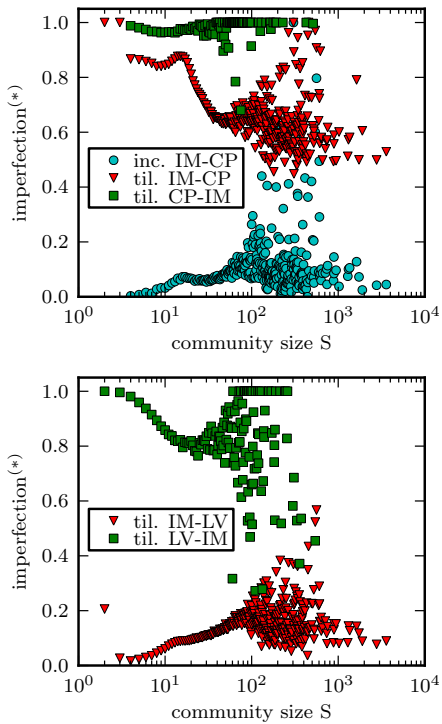


Figure 10: (Left) Tiling imperfection  $I$  and inclusion imperfection  $I^*$  between IM and CP. Open blue squares:  $I^*$  for tiling IM with CP; solid blue squares:  $I$  for tiling IM with CP; solid red squares:  $I$  for tiling CP with IM. (Right) Tiling imperfection  $I$  between IM and LV. Solid red squares:  $I$  for tiling IM with LV; solid blue circles:  $I$  for tiling LV with IM.

CP communities tend to “fit in” IM communities, this is likely because IM communities tend to extend far beyond CP communities and the majority of their nodes is thus outside the communities to be tiled.

However, for the IM-LV pair, the situation is different (Fig. 10b). The values for tiling imperfection are low for communities of all sizes, indicating that LV communities are often subgraphs of IM communities. It is worth noting that for small communities ( $S \lesssim 10$ ), the excessively low values of  $I$  indicate that the majority of IM communities can be perfectly tiled with LV communities. This is because the tiling imperfection  $I$  is quantized such that its values are integer fractions of the community size  $S$ . Hence e.g. for  $S = 5$ , the smallest attainable values are  $S = 0$  and  $S = 1/5$ , and as the displayed values are averages, almost every IM community of size  $S = 5$  is perfectly tiled with LV communities. In part, this tiling is due to the treelike nature of small IM and LV communities; furthermore, LV produces more small communities than IM, as seen in Fig. 2. A direct consequence of this is that LV communities can only be very poorly tiled with IM communities. The tiling between IM and LV is illustrated in Fig. 11.

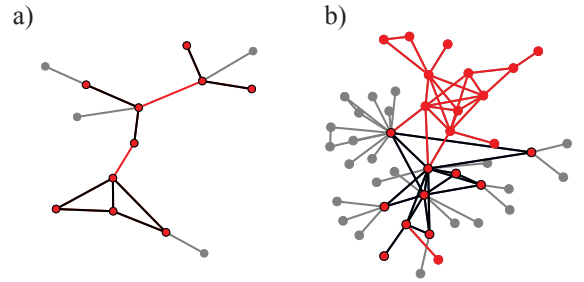


Figure 11: Typical cases of tiling with IM (red) and LV (black) communities of size  $S = 10$ . Gray nodes are the first neighbors of the community to be tiled. (a) Example of perfect tiling  $\mathcal{I} = 0$  when IM community (red nodes) is tiled with LV communities (black edges). A typical IM community with  $S = 10$  is located in a treelike region of the network, and LV covers such regions with very small communities. (b) Example of tiling imperfection  $\mathcal{I} = 1$  when LV community (black edges) is tiled with IM communities (in red). A typical LV community with  $S = 10$  is in a somewhat denser part of the network, where the IM communities are much larger.

## V. CONCLUSIONS AND DISCUSSION

We have applied three community detection methods on a large real-world social network and investigated the resulting communities. In earlier studies Infomap (IM) and the Louvain method (LV) have shown good performance on benchmark graphs [12, 13], while the benchmark results for clique percolation (CP) were worse. However, CP is known to be a fast method and capable of handling overlapping communities, and thus especially suitable for social networks.

For all the three methods, weighted or unweighted, the weights of edges inside communities were observed to be higher than the weights of edges between communities, in accordance with the Granovetter theory [37]. The distributions of community sizes were observed to be broad, as expected. For the partition-based methods, IM and LV, it was seen that small communities are often tree-like, which does not coincide well with the notion of a community in the context of social networks. This indicates that good performance on benchmark graphs does not assure meaningfully identified communities. When edge weights were taken into account, communities detected by the two partition-based methods were observed to become even sparser. When cross-comparing the community structures given by each method, the best overall match was between LV and IM, such that for small communities LV communities appeared to be subgraphs of IM communities. The match between CP and IM turned out to be considerably worse. However, this can be partially attributed to the tree-like character of many IM communities. In contrast CP clusters were always found in dense regions of the graph and in this sense meaningful *per se*, though it may happen that the strict requirements of clique percolation discard the important parts of com-

munities.

Benchmarks are helpful if the methods are to be tested for sensitivity to particular properties (such as hierarchical structure or broad distribution of cluster sizes). However, real-world networks are incomparably more complicated, e.g. they are often inhomogeneous in many respects and they may contain different kinds of mesoscopic structures. It may even happen that the same topological structure can be considered as a community for one purpose but not for another – an example is a star, which is by no means a community in the societal sense but may be reasonably considered as one for biochemical networks [31]. Our studies have shown that in large sparse networks the methods based on partitions inevitably identify some questionable regions as communities. This reflects a fundamental flaw in the underlying philosophy behind partition-based methods: it is assumed that networks are entirely built of communities, and hence each node must be assigned to one. Clearly, this is not the case. However, the tree-like formations and stars detected by IM and LV bear mesoscopic structural meaning: they, too, are important building blocks of the network. Hence, when analyzing large empirical networks, it is worth applying com-

plementary community detection methods and carefully compare the structural features of the resulting communities. In general, one might even argue that it would be beneficial to redirect the efforts on devising ever more efficient community detection methods towards a broader picture, by taking into account the existence of mesoscopic structures beyond communities.

### Acknowledgments

The project ICTeCollective acknowledges the financial support of the Future and Emerging Technologies (FET) programme within the Seventh Framework Programme for Research of the European Commission, under FET-Open grant number: 238597. We acknowledge support by the Academy of Finland, the Finnish Center of Excellence program 2006-2011, project no. 213470. JK thanks OTKA K60456 and TEKES for partial support. We thank Albert-László Barabási for the data used in this research.

- 
- [1] R. Albert, A.-L. Barabási, *Rev. Mod. Phys.* **74**, 47-97 (2002)
  - [2] M. E. J. Newman, *SIAM Review* **45**, 167-256 (2003)
  - [3] S. Boccaletti, V. Latora, Y. Moreno, M. Chavez and D. Hwang, *Physics Reports* **424**, 175 (2006)
  - [4] M. Newman, A.-L. Barabási, D. Watts: *The Structure and Dynamics of Networks* (Princeton University Press, 2006)
  - [5] G. Caldarelli, A. Vespignani (eds.): *Large Scale Structure and Dynamics of Complex Networks*, (World Scientific, 2007)
  - [6] R. Pastor-Satorras, A. Vespignani, *Phys. Rev. Lett.* **86**, 3200 (2001)
  - [7] J. D. Noh, H. Rieger, *Phys. Rev. Lett.* **92**, 118701 (2004)
  - [8] M. Barahona, L.M. Pecora, *Phys. Rev. Lett.* **89**, 054101 (2002)
  - [9] R. Milo, S. Shen-Orr, S. Itzkovitz, N. Kashtan, D. Chklovskii and U. Alon, *Science* **298**, 824 (2002)
  - [10] J.-P. Onnela, J. Saramäki, J. Kertész, K. Kaski, *Phys. Rev. E* **71**, 065103 (2005)
  - [11] S. Fortunato, *Phys. Reports* **486**, 75-174 (2010)
  - [12] A. Lancichinetti, S. Fortunato, F. Radicchi, *Phys. Rev. E* **78**, 046110 (2008)
  - [13] A. Lancichinetti, S. Fortunato, *Phys. Rev. E* **80**, 016118 (2009)
  - [14] M. Girvan, M. E. J. Newman, *Proc. Natl. Acad. Sci. (USA)* **99**, 7821 (2002)
  - [15] E. Ravasz, A. L. Somera, D. A. Mongru, Z. N. Oltvai, A.-L. Barabási, *Science* **297**, 1551-1555 (2002)
  - [16] M. E. J. Newman, M. Girvan, *Phys. Rev. E* **69**, 026113 (2004)
  - [17] U. Brandes, D. Delling, M. Gaertler, R. Goerke, M. Hofer, Z. Nikoloski, D. Wagner, *IEEE Trans. Knowl. Data Eng.* **20**, 172 (2008)
  - [18] J. Reichardt, S. Bornholdt, *Phys. Rev. E* **74**, 016110 (2006)
  - [19] R. Lambiotte, J.-C. Delvenne, M. Barahona, arXiv:0812.1770 (2008)
  - [20] S. Fortunato, M. Barthelemy, *PNAS* **104**, 36-41 (2007)
  - [21] J. M. Kumpula, J. Saramäki, K. Kaski, J. Kertész, *Eur. Phys. J. B* **56**, 41-45 (2007)
  - [22] G. Palla, I. Derényi, I. Farkas, T. Vicsek, *Nature* **435**, 814 (2005).
  - [23] G. Palla, A.-L. Barabási, T. Vicsek, *Nature* **446**, 664 (2007)
  - [24] M. Rosvall, C. T. Bergstrom, *PNAS* **104**, 7327 (2007)
  - [25] M. Rosvall, C. T. Bergstrom, *PNAS* **105**, 1118 (2008)
  - [26] F. Radicchi, C. Castellano, F. Cecconi, V. Loreto, D. Parisi, *PNAS* **101**, 2658 (2004)
  - [27] U. N. Raghavan, R. Albert, S. Kumara, *Phys. Rev. E* **76**, 036106 (2007)
  - [28] A. Lancichinetti, S. Fortunato, J. Kertész, *New J. Phys.* **11**, 033015 (2009)
  - [29] A. Lancichinetti, S. Fortunato, *Phys. Rev. E* **80**, 056117 (2009)
  - [30] V. D. Blondel, J.-L. Guillaume, R. Lambiotte, E. Lefebvre, *J. Stat. Mech.* P10008 (2008).
  - [31] A. Lancichinetti, M. Kivelä, J. Saramäki, S. Fortunato, arXiv:1005.4376 (2010).
  - [32] R. Pastor-Satorras, A. Vázquez, A. Vespignani, *Phys. Rev. Lett.* **87**, 258701 (2001)
  - [33] R. Milo, S. Itzkovitz, N. Kashtan, R. Levitt, S. Shen-Orr, I. Ayzenshtat, M. Sheffer, U. Alon, *Science* **303**, 1538 (2004)
  - [34] Y.-Y. Ahn, J. P. Bagrow, and S. Lehmann, arXiv:0903.3178 (2009)
  - [35] J.-P. Onnela, J. Saramäki, J. Hyvönen, G. Szabó, D. Lazer, K. Kaski, J. Kertész, and A.-L. Barabási, *Proc.*

- Natl. Acad. Sci. (USA)* **104**, 7332 (2007)
- [36] J.-P. Onnela, J. Saramäki, J. Hyvönen, G. Szabó, M. A. de Menezes, K. Kaski, A.-L. Barabási, and J. Kertész *New J. Phys.* **9**, 179 (2007)
- [37] M. Granovetter, *Am. J. Sociol.* **78**, 1360 (1973)
- [38] <http://sites.google.com/site/findcommunities/>
- [39] <http://www.tp.umu.se/~rosvall/code.html>
- [40] <http://cfinder.org/>
- [41] M. Granovetter: Getting a Job: A Study of Contacts and Careers *University of Chicago Press*, 2005
- [42] I. Farkas, D. Ábel, G. Palla, T. Vicsek, *New J. Phys.* **9**, 180 (2007)
- [43] J.M. Kumpula, J.M. Kumpula, M. Kivelä, K. Kaski, and J. Saramäki, *Phys. Rev. E* **79**, 026109 (2008)
- [44] A. Clauset, M.E.J. Newman and C. Moore, *Phys. Rev. E* **70**, 066111 (2004)